Published in: Bentz, D.P., Halleck, P.M., Grader, A.S., and Roberts, J.W., "Four-Dimensional X-ray Microtomography Study of Water Movement during Internal Curing," in Proceedings of the International RILEM Conference – Volume Changes of Hardening Concrete: Testing and Mitigation, Eds. O.M. Jensen, P. Lura, and K. Kovler, RILEM Publications S.A.R.L., Bagneux, France, 11-20,2006.

Four-Dimensional X-ray Microtomography Study of Water Movement during Internal Curing

Dale P. Bentz
Materials and Construction Research Division
National Institute of Standards and Technology
100 Bureau Drive Stop 8615
Gaithersburg, MD 20899-8615 USA
E-mail: dale.bentz@nist.gov

Phillip M. Halleck and Abraham S. Grader
Center for Quantitative Imaging
The Pennsylvania State University
152 Hosler Building
University Park, PA 16802-5000 USA
E-mail: phil@pnge.psu.edu

John W. Roberts
Northeast Solite Corporation
1500 Westbrook Ct., Apt. 5115
Richmond, VA 23227
E-mail: johnsolite@aol.com

Abstract

While the effectiveness of internal curing has been verified via a variety of experimental measurements, including internal relative humidity, autogenous shrinkage, restrained shrinkage, strength development, and degree of hydration, a direct observation of water movement during internal curing in **four dimensions** (three spatial dimensions and time) has been lacking. X-ray microtomography offers the possibility to dynamically monitor density changes in a material, during its curing process, for example. In this paper, this technique is applied to monitoring water movement from saturated lightweight aggregate particles to the surrounding hydrating cement paste in a high performance mortar mixture over the course of the first 2 d of hydration at 30 ^{o}C. A four-dimensional data set is created by obtaining three-dimensional image sets on a single specimen after various hydration times, from just after mixing to after 47 h of hydration, with a voxel dimension of less than 20 μm, allowing a clear delineation of individual lightweight aggregate particles and much of their internal porosity. Many of the changes in local density, corresponding to water movement, occur during the first 24 h of hydration, during the acceleratory period of the cement hydration reactions. The four-dimensional data set is processed and analyzed to quantitatively estimate the volume of internal curing water that is supplied as a function of hydration time. These microtomography-based observations of water movement are supported by more conventional measurements of hydration including non-

evaporable water content via loss-on-ignition, chemical shrinkage, and heat of hydration via isothermal calorimetry.

Introduction

The goal of internal curing is to maintain saturated conditions within a hydrating cement paste in order to avoid self-desiccation and the accompanying autogenous stresses and strains that may lead to early age cracking. The effectiveness of internal curing, using saturated lightweight aggregates (LWA) or superabsorbent polymers (SAP), for example, has been evaluated based on the measurement of a wide variety of performance properties, including internal relative humidity, autogenous shrinkage, restrained shrinkage and creep, degree of hydration, and compressive strength development [1-4]. All of these measurements have indicated that the internal reservoirs (SAP or LWA) can be an effective means for supplying the extra curing water needed to compensate for the chemical shrinkage occurring in the cement paste during hydration. Still, it is desirable to make an even more direct observation of the water movement from the internal reservoirs to the surrounding cement paste during hydration.

X-ray absorption is one non-destructive technique that can be used to probe the dynamic microstructure of porous materials such as cement pastes and mortars [5-8]. In the past, x-ray transmission measurements have been used to investigate water movement during early age curing/drying of small cement paste and mortar specimens as a function of water-to-cement ratio (*w/c*), cement particle size distribution, curing conditions, and the addition of a shrinkage-reducing admixture [5-7]. Lura et al. [8] have also applied the x-ray transmission technique to investigating water movement from a single saturated LWA to cement paste during hydration, successfully comparing the estimated water movement to the measured (and modeled) chemical shrinkage of the cement paste under equivalent hydration conditions. However, due to the resolution limit of about 100 μm of the x-ray absorption equipment employed in that study and its inability to operate in a tomography mode, only the "bulk" movement of water could be estimated. X-ray microtomography [9, 10] offers the possibility to perform similar measurements on an entire specimen and isolate water movement from individual "pores" in the LWA to the surrounding cement paste during hydration. Such an experiment has been summarized recently [11]; here, a more detailed quantitative analysis of the water movement based on image processing and analysis of the four-dimensional image set will be presented.

Experimental

Many of the experimental details have been provided in reference [11], so that only a brief summary will be provided here. The high performance mortar with internal curing was proportioned according to the methodology outlined in [12], using a Type I/II portland cement and a mixture of four normal weight sands in addition to the saturated lightweight sand. The *w/c*=0.35 mortar for the microtomography experiment was prepared at the microtomography laboratory. An air content of 2.1 % by volume fraction was measured for the fresh mortar based on a unit mass measurement, using specific gravities of 3.22, 2.61, and 1.7 for the cement powder, normal weight sand, and saturated surface dried LWA, respectively. A small sample of the mortar was carefully compacted into a 13 mm inner diameter by 42 mm high plastic tube that was subsequently sealed inside of a larger 27 mm diameter polypropylene tube in which a cooling fluid was constantly circulated to maintain a temperature of 30 ^{o}C. Following sample

preparation, the specimen in its holder was placed inside the x-ray equipment, where it remained basically stationary throughout the 2 d of the experiment.

Volumetric x-ray CT data were collected using the facility's microfocus x-ray source with a voltage setting of 120 kV and a tube current of 200 μA, to minimize the focal spot size (≈ 10 μm) and thus optimize the spatial resolution. For this study, all of the microtomography data sets were acquired with voxel dimensions of dx = dy = 18 μm and dz = 19 μm, each of which is larger than the focal spot size quoted above. Each data set consisted of a 1024 x 1024 x 246 array of 16-bit x-ray absorption values on an arbitrary scale. Each of the 246 individual two-dimensional slices was available as a 16-bit tiff-format image for further processing and analysis as described below.

The microtomography experiment was accompanied by supporting measurements on cement paste and mortar specimens of non-evaporable water content via loss-on-ignition (LOI), chemical shrinkage [13], and heat of hydration via isothermal calorimetry at 30 ^{o}C, in order to compare the water supplied via internal curing to the hydration rates as assessed by these three complementary experimental techniques [14, 15]. Non-evaporable water content was determined as the mass loss between 105 ^{o}C and 1000 ^{o}C, corrected for the LOI of the starting materials (cement and sands), with estimated expanded uncertainties of 0.004 and 0.01 for pastes [7, 15] and mortars [16], respectively. Chemical shrinkage measurements were conducted according to the ASTM C1608 standard [13], with an expected precision of 0.0042 (g water/g cement). Isothermal calorimetry was conducted using a conventional differential scanning calorimeter (DSC) with a sample (cement paste) mass of about 120 mg. For temperatures between -100 ^{o}C and 500 ^{o}C, the DSC manufacturer has specified a constant calorimetric sensitivity of ± 2.5 %, with a root-mean-square baseline noise of 1.5 μW.

Results

Figures 1 to 3 provide two-dimensional and three-dimensional images of the raw microtomography data sets and of the results of subtracting the original data set from that obtained after 1 d of hydration. In the two-dimensional images in Figure 1, the specimen is seen to contain four readily distinguishable phases based on differences in density (or more correctly x-ray absorption): dark air voids and empty pores (within LWA particles), dark grey LWA particles and water-filled pores within the LWA, light grey sand particles, and bright cement paste. Some empty pores are observed within the LWA particles even in the image set obtained immediately after mixing, suggesting that either these pores were not saturated by the saturation procedure employed in this study or that they had emptied during the initial mixing and casting of the specimen. In carefully comparing the original 2-D slice to that obtained after 1 d or 2 d of hydration, for several of the (circled) LWA particles, one can notice a general darkening and the appearance of new (empty) pores within the particles in the latter images. These correspond to initially water-filled pores that were emptied to supply internal curing water to the surrounding cement paste during its hydration. These emptied pores are highlighted in aqua in the lower right image of Figure 1 and in Figures 2 and 3. All three of these images were obtained by subtracting the original image set from that obtained after 1 d of hydration. The sizes and shapes of many of the "individual" pores (or porous regions) within the LWA particles are readily observed, both in their two-dimensional (Figures 1 and 3) and in their three-dimensional (Figure 2) forms. Most of these empty pores were created during the first day of hydration, with little further change being observed between the 1 d and 2 d hydrated image sets.

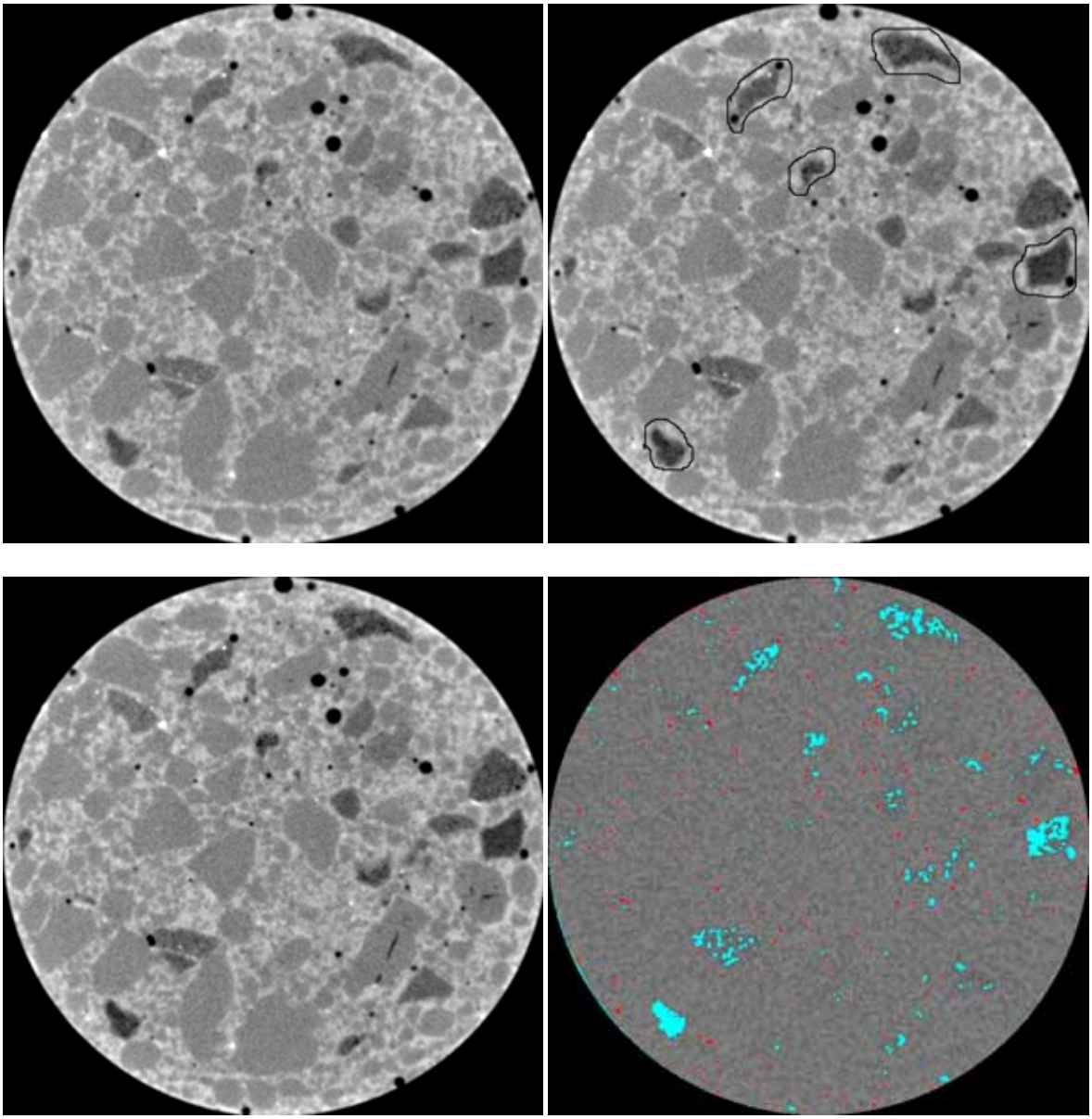

Fig. 1: Two-dimensional slices (13 mm x 13 mm) from 3-D microtomographic data sets corresponding to: upper left- mortar immediately after mixing, upper right – mortar after about 1 d of hydration, lower left – mortar after about 2 d of hydration, and lower right – subtracted color-coded image of 1 d - original slices. In the color-coded image, aqua indicates regions of drying and red indicates regions of wetting [11].

To perform a more detailed quantitative analysis of the volume of water moving from the saturated LWA to the hydrating cement paste, each three-dimensional image set was processed and analyzed as follows. First, to reduce the random noise present in the three-dimensional image sets, each image was processed using a median filter. In applying a median filter, each voxel (image element) within the specimen volume is replaced by the median (greylevel) value for all voxels within a fixed size cube centered on the voxel being considered. Median filters remove noise by smoothing the data, but while preserving small details and sharp edges [17]. For this study, 3 voxel x 3 voxel x 3 voxel and 5 voxel x 5 voxel x 5 voxel cubes were

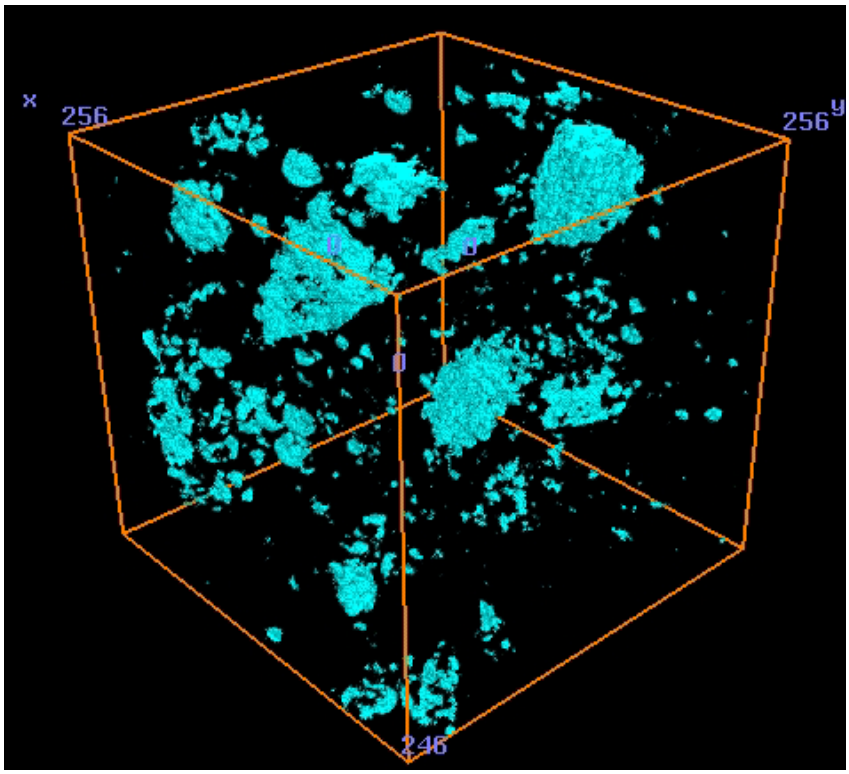

Fig. 2: Three-dimensional color-coded image of original data set subtracted from that obtained after 1 d of hydration. Aqua volumes indicate regions where the LWA particles have lost water (to the surrounding hydrating cement paste). 3-D volume is 4.6 mm x 4.6 mm x 4.7 mm [11].

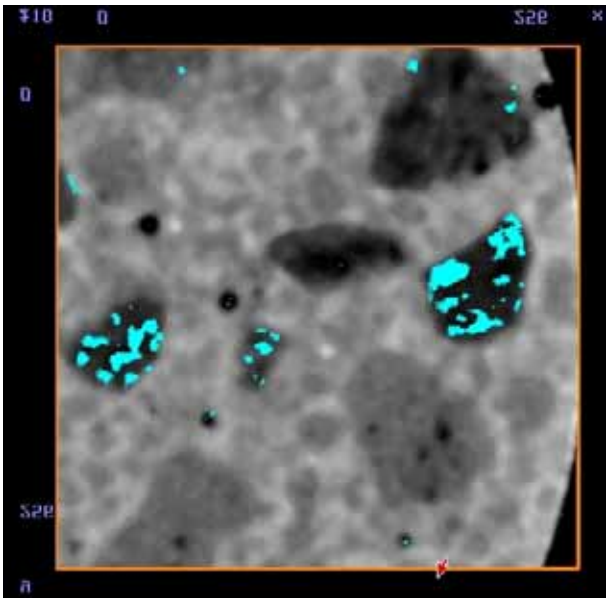

Fig. 3: Two-dimensional image (4.6 mm x 4.6 mm) of a portion of the original mortar microstructure with the locations of the evacuated water (in aqua) superimposed [11].

investigated. After filtering, the greylevel histogram (a plot of the number of voxels containing each greylevel intensity value vs. greylevel intensity) was determined for each (original and processed) data set. Representative histograms are provided in Figure 4 for the data set obtained

after 2 d of hydration. Peaks in a greylevel histogram usually indicate individual phases within a microstructure and the sharpening of the peaks in the median-filtered image sets relative to the original data set is clearly observed in Figure 4. Based on its greater separation into individual peaks, the 5 voxel x 5 voxel x 5 voxel median-filtered data sets were selected for further analysis. In Figure 4, the "peaks" corresponding to each of the four detectable phases listed above are labeled with their corresponding name (pores, LWA, sand, and paste).

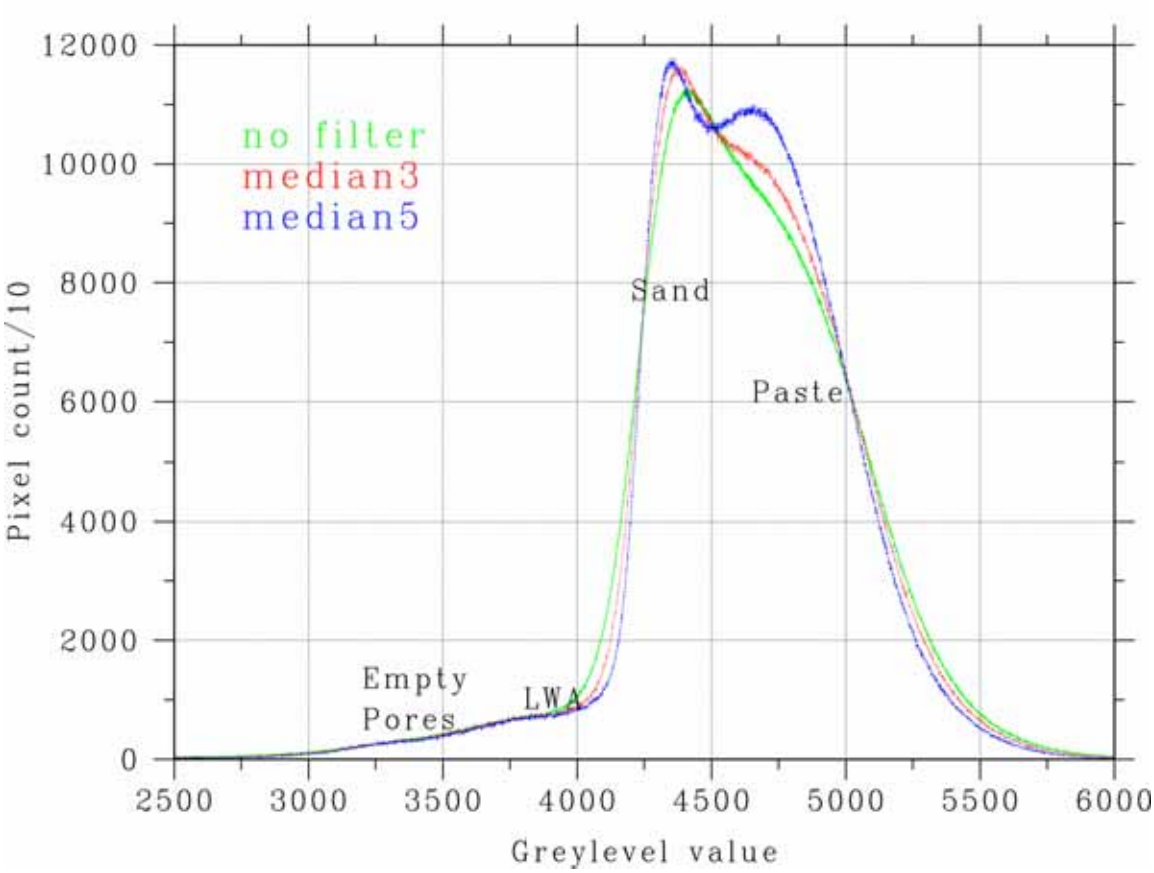

Fig. 4: Greylevel histograms for three-dimensional image set obtained after 2 d of hydration, subjected to different size (three-dimensional) median filters.

Figure 5 presents the greylevel histograms for the original, 1 d, and 2 d hydration image sets, after applying the 5 voxel x 5 voxel x 5 voxel median filter to each. The differences in the histograms as a function of hydration time should now correspond to the changes occurring within the specimen microstructure (mainly water movement from the LWA to the surrounding cement paste). The effects of the water movement are three-fold: 1) an increase in the number of voxels detected as empty pores, 2) a decrease in the number of voxels detected as (water-filled) LWA, and 3) an increase in the brightness of the voxels containing hydrating cement paste (due to the density and x-ray absorption increase accompanying the water imbibition into the hydrating porous microstructure) as indicated by the three greylevel histogram curves crossing one another at a greylevel value of about 5000 in Figure 5. Here, the first of these will be used to estimate the cumulative volume fraction of internal curing water that has moved from the LWA reservoirs to the surrounding paste, corresponding to the volume of created empty pores. To do this, the integral of the greylevel histogram is computed for the darkest (lowest intensity) subset

of greylevels, specifically between 0 and an upper limit that defines the greylevel boundary between empty pores (both air voids and empty pores within the LWA) and water-filled pores/LWA particles. For the analysis conducted here, this upper limit was set both at 3500 (corresponding to the presence of a slight shoulder in the greylevel histograms in Figure 5) and at 3900 (corresponding to the point where the 1 d and original histograms cross each other indicating an increase in empty pores and a decrease in water-filled ones). For example, the number of voxels with intensities less than 3900 was determined for each median-filtered image set and divided by the total number of voxels within the three-dimensional specimen volume to obtain a volume fraction.

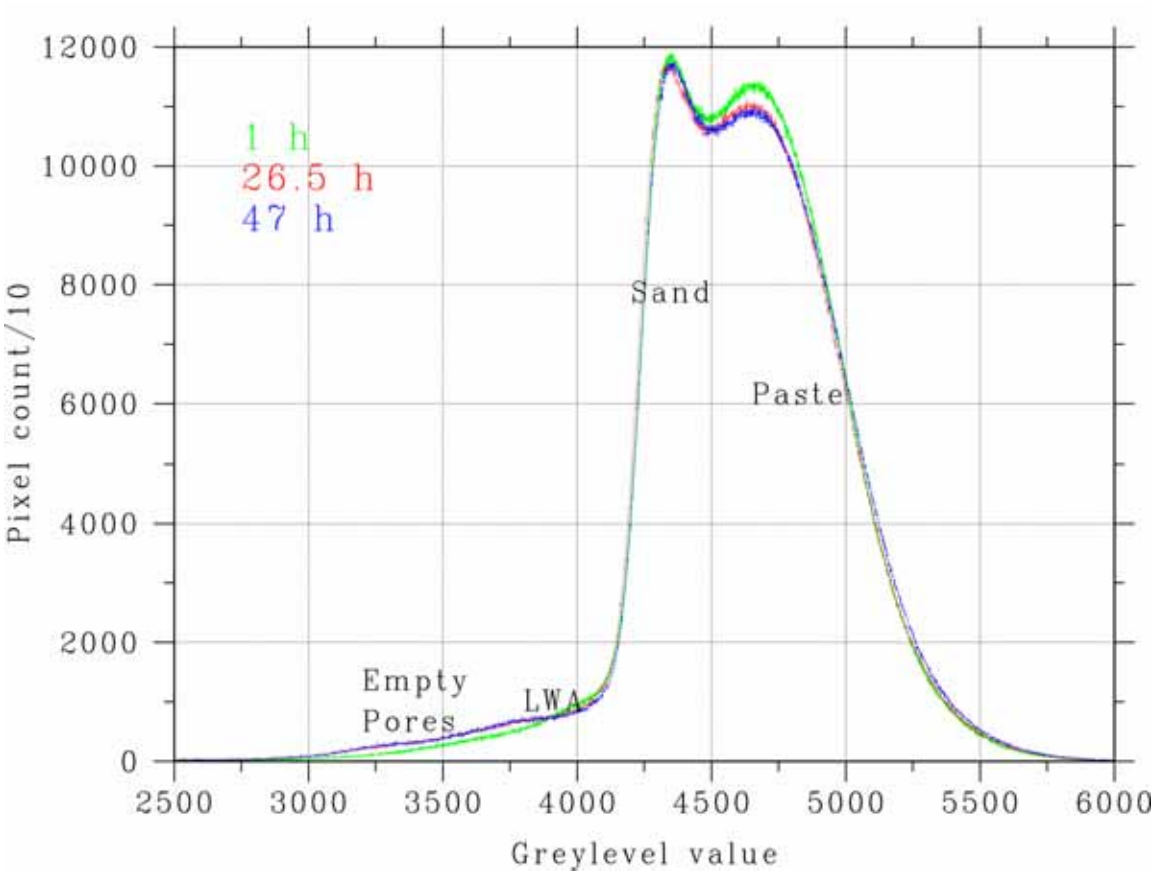

Fig. 5: Greylevel histograms for three-dimensional image sets (median filtered) obtained immediately after mixing, after 1 d, and after 2 d of hydration.

In Figure 6, these volume fractions are plotted against hydration time and compared to more conventional measures of hydration such as cumulative heat release, degree of hydration based on LOI, and chemical shrinkage (in units of milliliter of imbibed water per milliliter of mortar). The initial volume fraction of voxels with greylevel intensities less than 3900 (about 2.8 %) is seen to be in reasonable agreement with the measured air void content of the fresh mortar (2.1 %), considering that the image-based measurement also includes some empty pores within the LWA in addition to the air voids. The shape of the curves for the volume of water removed from the LWA during the first day of internal curing is seen to closely follow the shape of the curves for the degree of hydration of the specimen as determined by the three different analytical methods. This suggests that for this LWA system, the needed curing water is readily

available to the hydrating cement paste during the first few days of hydration. A more direct comparison of the volume fraction of "emptied LWA" voxels to the volume fraction of imbibed water (chemical shrinkage) of an equivalent saturated cement paste is provided in Figure 7. Because the volume fraction of "emptied" voxels is only a lower bound on the volume of water moving from the LWA to the hydrating cement paste, due to the emptying of water-filled pores that are smaller than the resolution limits of the tomographic data sets, etc., in Figure 7, the emptied voxels volume fraction vs. time has been scaled to match exactly the 24 h measured chemical shrinkage data. With this scaling, Figure 7 shows a virtual one-to-one agreement between the measured volume of imbibed water and the scaled measured volume of emptied pores during the first 36 h of the experiment.

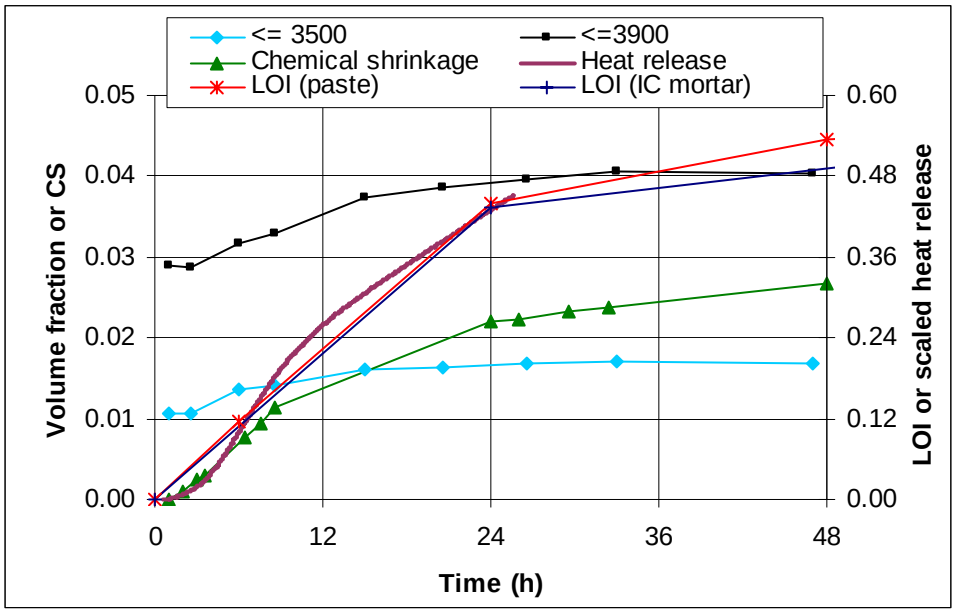

Fig 6: Estimated curing water supplied vs. time in comparison to other conventional measurements of hydration.

It should be noted that while the individual pores being emptied within the LWA particles are readily identified (e.g., in Figure 1), individual "locations" within the hydrating cement paste to which this water is moving could not be reliably detected in this experiment. At these early ages, the water from the LWA readily moves distances of 5 mm or more from its source [5, 6, 8] so that the internal curing water is more or less homogeneously distributed throughout the three-dimensional microstructure. In this study, the mortar was proportioned with enough internal curing water to satisfy the hydration demand only during the first 48 h of hydration, as it was envisioned to freeze the specimen after 2 d and hopefully observe water/ice movement from the hydrating cement paste to the air voids and (now) empty pores within the LWA particles. Unfortunately, we were only able to achieve a specimen temperature of about -8 ^{o}C during this freezing, such that the water within the porous hydrating cement paste may not have frozen due to supercooling effects.

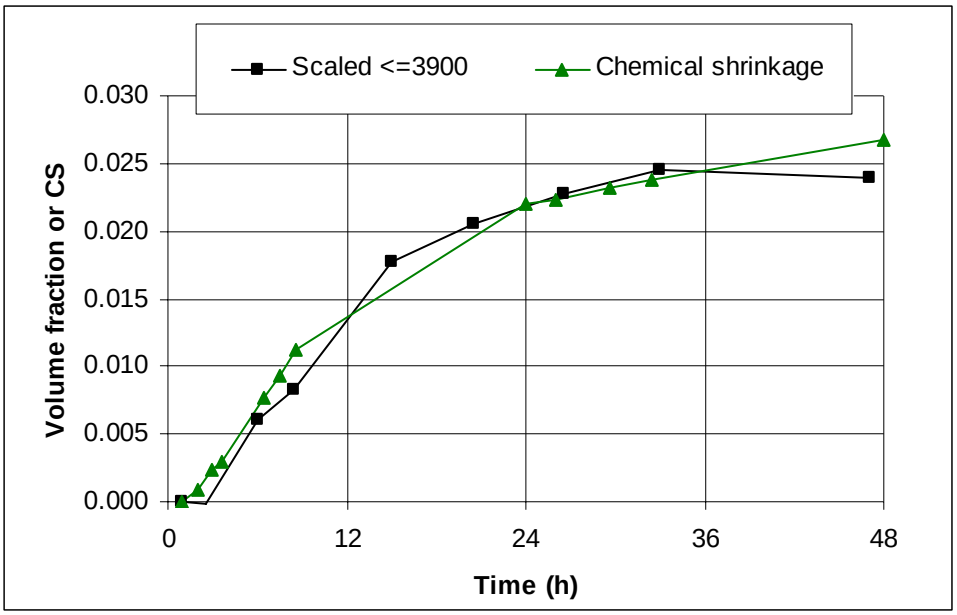

Fig 7: Comparison of measured chemical shrinkage volume fraction to scaled (see text) emptied LWA pore volume fraction vs. curing time.

Conclusions

X-ray microtomography was successfully applied to observing water movement from saturated LWA to the surrounding cement paste during hydration. Following the application of a 5 voxel x 5 voxel x 5 voxel median filter to each acquired three-dimensional image set, the volume of internal curing water supplied to the paste as a function of time was readily estimated, based on analysis of each specimen's greylevel histogram. This estimated volume of curing water closely followed the same trends as the degree of hydration measured by three different techniques (LOI, chemical shrinkage, and isothermal calorimetry). For this particular mortar, much of the water movement occurred during the first 24 h of hydration, emphasizing the importance of proper early-age curing. In the future, it would be of interest to repeat the freezing portion of this study by cooling the specimen to about -20 ^{o}C, at which temperature freezing within the porous cement paste microstructure should definitely occur.

Acknowledgements

The authors would like to thank Mr. Max Peltz and Mr. John Winpigler of the Building and Fire Research Laboratory at the National Institute of Standards and Technology for their assistance with materials characterization and specimen preparation. They would also like to thank Mr. Jeffrey Hook of the Lehigh Portland Cement Company for supplying materials for this study and Dr. Pietro Lura of the Technical University of Denmark for useful discussions.

References

1. Geiker, M.R., Bentz, D.P., and Jensen, O.M., "Mitigating Autogenous Shrinkage by Internal Curing," *High Performance Structural Lightweight Concrete*, ACI SP 218, J.P. Ries and T.A. Holm, eds. American Concrete Institute, Farmington Hills, MI, 2004, pp. 143-154.

2. Jensen, O.M., and Hansen, P.F., "Water-Entrained Cement-Based Materials II: Experimental Observations," *Cement and Concrete Research*, V. 32, No. 6, 2002, pp. 973-978.

3. Cusson, D., and Hoogeveen, T., "Internally-Cured High-Performance Concrete Under Restrained Shrinkage and Creep," CONCREEP 7 Workshop on Creep, Shrinkage and Durability of Concrete and Concrete Structures, Nantes, France, Sept. 12-14, 2005, pp. 579-584.

4. Cusson, D., Hoogeveen, T., and Mitchell, L.D., "Restrained Shrinkage Testing of High-Performance Concrete Modified with Structural Lightweight Aggregate," 7th International Symposium on Utilization of High-Strength/High-Performance Concrete, Washington, USA, June 2005, 20 pp.

5. Bentz, D.P., and Hansen, K.K., "Preliminary Observations of Water Movement in Cement Pastes During Curing Using X-ray Absorption," *Cement and Concrete Research*, V. 30, 2000, pp. 1157-1168.

6. Bentz, D.P., Hansen, K.K., Madsen, H.D., Vallee, F.A., and Griesel, E.J., "Drying/Hydration in Cement Pastes During Curing," *Materials and Structures*, V. 34 2001, pp. 557-565.

7. Bentz, D.P., Hansen, K.K., and Geiker, M.R., "Shrinkage-Reducing Admixtures and Early Age Desiccation in Cement Pastes and Mortars," *Cement and Concrete Research*, V. 31, No. 7, 2001, pp. 1075-1085.

8. Lura, P., Bentz, D.P., Lange, D.A., Kovler, K., Bentur, A., and van Breugel, K., "Measurement of Water Transport from Saturated Pumice Aggregates to Hardening Cement Paste," accepted by *Materials and Structures,* 2006.

9. Bentz, D.P, Mizell, S., Satterfield, S., Devaney, J., George, W., Ketcham, P., Graham, J., Porterfield, J., Quenard, D., Vallee, F., Sallee, H., Boller, E., and Baruchel, J., "The Visible Cement Data Set," *Journal of Research of the National Institute of Standards and Technology*, V. 107, No. 2, 2002, pp.137-148.

10. Landis, E.N., Zhang, T., Nagy, E.N., Nagy, G., and Franklin, W.R., "Cracking, Damage, and Fracture in Four Dimensions," accepted by *Materials and Structures*, 2006.

11. Bentz, D.P., Halleck, P.M., Grader, A.S., and Roberts, J.W., "Direct Observation of Water Movement during Internal Curing Using X-ray Microtomography," *Concrete International*, V. 28, No. 10, 2006, pp. 39-45.

12. Bentz, D.P., Lura, P., and Roberts, J.W., "Mixture Proportioning for Internal Curing," *Concrete International*, V. 27, No. 2, 2005, pp. 35-40.

13. ASTM C1608-05, "Test Method for the Chemical Shrinkage of Hydraulic Cement Paste," ASTM International, West Conshohocken, PA, 2005.

14. Parrott, L.J., Geiker, M., Gutteridge, W.A., and Killoh, D., “Monitoring Portland Cement Hydration: Comparison of Methods,” *Cement and Concrete Research*, V. 20, 1990, pp. 919-926.

15. Bentz, D.P., "Three-Dimensional Computer Simulation of Cement Hydration and Microstructure Development," *Journal of the American Ceramic Society*, V. 80, No. 1, 1997, pp. 3-21.

16. Bentz, D.P., “Capitalizing on Self-Desiccation for Autogenous Distribution of Chemical Admixtures in Concrete,” *Proceedings of the 4th International Seminar on Self-Desiccation and Its Importance in Concrete Technology*, B. Persson, D.P. Bentz, and L.-O. Nilsson, eds., Lund University, Lund, Sweden, 2005, pp. 189-196.

17. Marion, A., An Introduction to Image Processing, Chapman and Hall, London, 1991.